Chapter 9

Atmospheric Attenuation of the Terahertz Wireless Networks

Milda Tamosiunaite, Stasys Tamosiunas, Mindaugas Zilinskas and Gintaras Valusis

Additional information is available at the end of the chapter

http://dx.doi.org/10.5772/intechopen.72205

Abstract

The increase of data traffic, a demand for high-speed reliable mobile networks and congested frequency bands raised both technological and regulatory challenges. Therefore, the fifth-generation mobile network (5G) is being developed. Recently, researchers have focused on a very promising terahertz (THz) band (frequencies from 100 GHz to 30 THz), which will allow fast transmission of huge amounts of data. However, transmission distance is limited due to atmospheric attenuation, as THz waves undergo significant absorption by water vapor and oxygen molecules in the atmosphere. Moreover, THz waves are very vulnerable by precipitation. Furthermore, the path of the propagating waves changes due to variations of the atmospheric refractive index. Nevertheless, the THz networks could be perfect candidates for fiber-to-THz bridges in difficult-to-access areas. The aim of this chapter is to present the possibilities and challenges of the THz networks from a point of view of atmospheric attenuation. The results show that simulations of the atmospheric attenuation using real-time data are a powerful tool that should complement technological basis, as it will help to foresee possible failures, extend transmission distance and improve reliability of the THz and other high-frequency broadband wireless networks.

Keywords: broadband wireless communications, terahertz wireless networks, atmospheric attenuation, rain attenuation, refractive index

1. Introduction

Data traffic in wireless communications has been increasing rapidly over recent decades. Edholm's law (resembling the well-known Moore's law for transistors) states that wireless data rates have doubled every 18 months over the last three decades and are quickly

approaching the capacity of wired communication systems [1]. Furthermore, the Internet traffic is expected to reach over 130 exabytes per month by 2018 [2]. The speed limits are based on the Shannon theorem [3], which states that, for a given average signal power, the channel bandwidth limits the maximum data rate that can be attained with a sufficiently low error rate.

The most desirable spectrum to satisfy the wireless needs is the frequency band of 1–10 GHz, whereas propagation losses due to atmospheric absorption and precipitation play a secondary role, and in many cases may generally be neglected[1] [4]. However, the band up to 10 GHz is highly congested. Despite the efforts to improve its efficiency, it is difficult to locate a sufficient amount of free bandwidth. Since current networks are no longer able to cope with the forthcoming load (i.e., Internet of Things (IoT), self-driving cars and so on), recent research has focused on the THz technology, which has a lot of potential owing to a large bandwidth capability, highly directive beams, obtained with relatively small antennas, and, consequently, low transmitter power requirement. Although transmission distance will be limited due to severe effects in the atmosphere, the THz networks are perfect candidates for short-distance communications, such as fiber-to-THz bridges in difficult-to-access areas.

The aim of this chapter is to present the possibilities and challenges of the THz networks from a point of view of atmospheric attenuation. The chapter consists of three parts. The first part is dedicated to the review of the possible applications and basic concepts of the THz wireless networks. In the second part, the main mechanisms of the atmospheric attenuation are presented. This part also includes a brief overview of the basic principles of radio system design and recommendations of the International Telecommunication Union (ITU-R). The third part is based on real-time measurements and simulations using meteorological data.

2. Terahertz wireless networks

2.1. The terahertz band

The terahertz (THz) band (also often called the T-rays or „terahertz gap") consists of electromagnetic waves in the frequency region of 100 GHz–30 THz.[2] One terahertz (1 THz = 10^{12} Hz) corresponds to a vacuum wavelength of 0.3 mm. As terahertz radiation begins at a wavelength of 1 mm and proceeds into shorter wavelengths, it is sometimes called the submillimeter band. The THz band is also called the "terahertz gap," as it divides the microwaves and infrared waves or, in other words, the electronics and optics (**Figure 1**). Both electronics and optics contributed to the development of the THz technology, as photonics has led the way to the realization of many important THz devices, such as the development of the quantum cascade laser (QCL), while electronics contributed with solid-state electronic devices, such as resonant tunneling diodes (RTD) [5].

[1]However, the application cannot be so straightforward. In order to ensure a reliable connection, the attenuation of the atmosphere should be evaluated starting from 1 GHz or even lower frequency.

[2]100 GHz corresponds to 0.1 THz. Perspectives for telecommunications are expected in the region up to 10 THz.

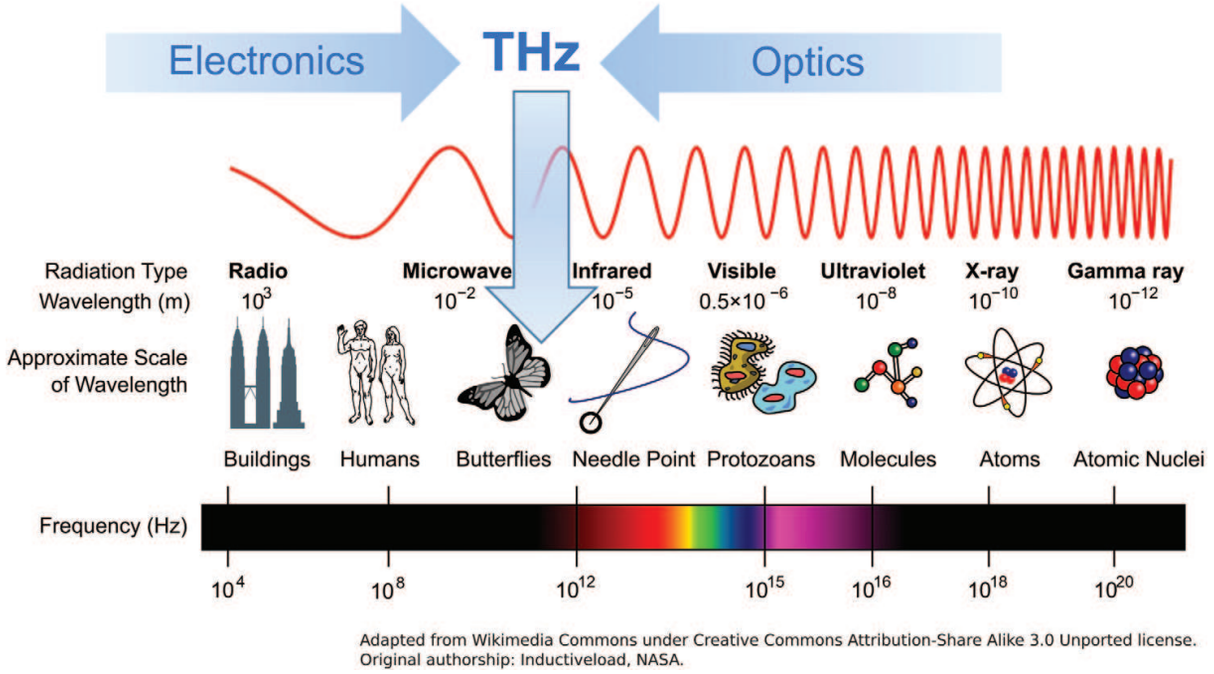

Figure 1. The terahertz (THz) gap. Both electronics and photonics contributed to the development of the THz technology.

The THz band, combined with recent technological innovations, offers wide application possibilities from nondestructive medical imaging, quality control, security issues (i.e., detection of weapons, explosives and narcotic substances, as every material has a distinct signature in its THz spectra [6]), communications and many more. The communication sector can benefit from THz technology in many ways, starting from wireless communications and high-speed data processing, to satellite communications.

2.2. The concept of ultrabroadband THz wireless networks

According to [7], there are several reasons that motivate the use of the THz band for ultrabroadband communication networks. First of all, wireless technologies below 0.1 THz (100 GHz) are not able to support terabit per second (Tbps) links, as available bandwidth limits the achievable data rates (however, compact wireless technologies above 10 THz are not able to support Tbps links). Furthermore, the THz band offers a much larger bandwidth, which ranges from tens of GHz up to several THz, depending on the transmission distance, and it opens the door for the variety of applications that demand ultrahigh data rates. In 2012, a group of researchers have smashed the record for wireless data transmission in the terahertz band. The data rate was 20 times higher than the best commonly used Wi-Fi standard [8]. However, due to technological limitations, the best performance of the THz wireless network is shown under indoor conditions. One of the main challenges is a very high path loss at THz band frequencies, which limits the communication distances[3] [7]. The appropriate frequency band should be determined by the application [9], as the higher the operational frequency,

[3]In addition to all the challenges, the THz Band is not yet regulated. However, the beginning development is accompanied by standardization activities addressing the lower THz range. According to the proposal of the IEEE 802.15.3 group, the frequency range 252–325 GHz is defined as the Thz PHY, and the links using Thz PHY are called THz links.

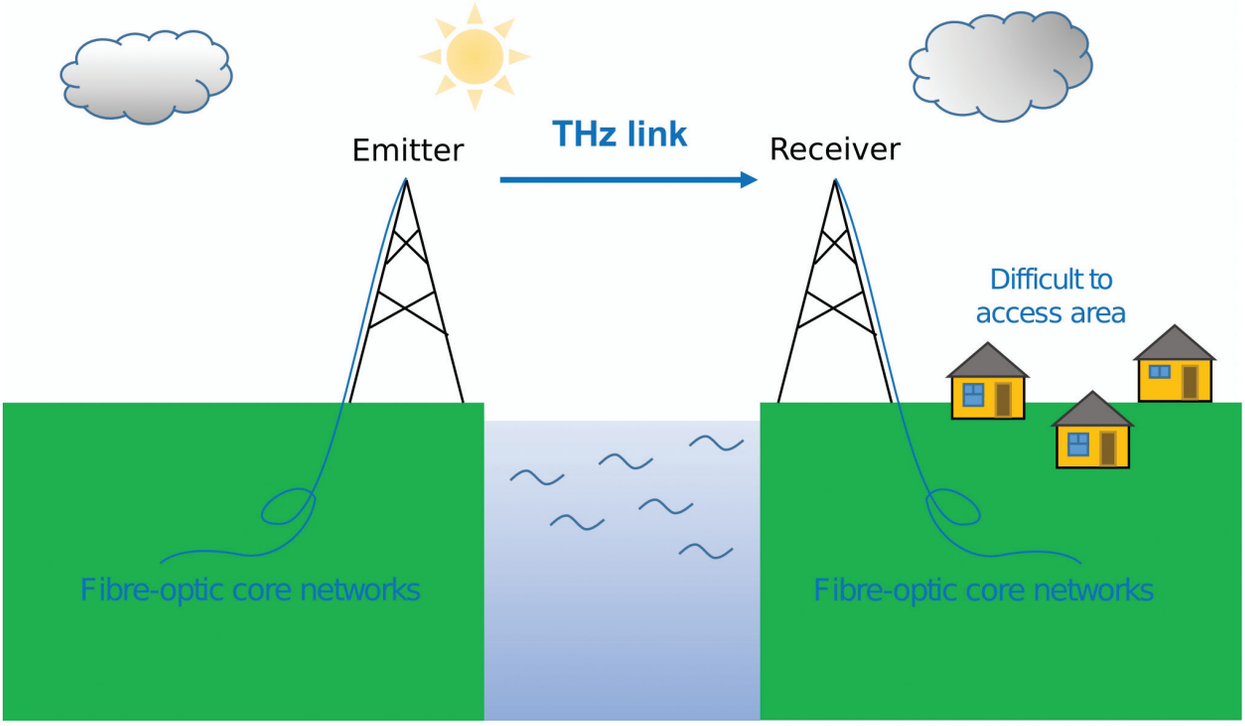

Figure 2. The concept of fiber-to-THz radio bridges for connection between a fiber-optic link and a THz link.

the shorter the distance (~100–150 GHz for long distance (~1–10 km), <350 GHz for medium distance (~100 m–1 km) and <500 GHz for indoor (~10–100 m) communications) which THz wave can travel without crucial distortions. Bearing in mind the distance problem, THz communications could benefit from the well-developed fiber-optic links. The wireless-over-fiber technology was introduced in [10]. In fact, owing to low losses in the optical fiber cables for long-haul transmission, wireless-over-fiber is a very promising technology for the difficult-to-access areas (**Figure 2**). In addition, the basic principles of the 5G technology can be adapted, such as the massive Multiple Input, Multiple Output (MIMO) antennas integrated into base stations [11] and densely deployed small cells [12] that are able to maintain a decent level of signal quality in areas with high density of mobile users [13]. Other solutions are also possible. For example, in [14], a concept of mirror-assisted wireless coverage system is suggested. The smart antennas are utilized with a number of moveable dielectric mirrors that act as reflectors for the THz waves, creating a virtual line of sight.

However, as was concluded in [15], the transmission capacity of a system with a given transmission power depends critically on channel properties like path losses, antenna misalignment and interference due to reflection and scattering.

3. Propagation modeling (atmospheric attenuation)

The design techniques of the new telecommunication links take into account a series of various factors that are comprehensively explained by Freeman [4] and regulated by the International Telecommunication Union (ITU-R). If a beam would propagate in free space

without atmosphere, the path would be a straight line. However, the atmosphere is always present. In this chapter, the atmospheric effects on propagation are briefly overviewed in terms of the THz communications. A more detailed description of the atmospheric effects is provided in [16].

3.1. Free-space loss vs. actual atmosphere

A free-space path loss (FSPL) is inevitable attenuation in the line-of-sight path through free space. In general case, the free-space loss rises with the square of the carrier frequency and link distance (i.e., 100 dB for a 10-m THz link at a carrier frequency of 300 GHz [17]). In actual atmosphere, there are additional sources of atmospheric loss that affects the amplitude, phase and polarization of electromagnetic waves. Generally, these effects could be predicted. The prediction procedures consist of few steps, and the meteorological data (rain rate, temperature, humidity, etc.) are required.

3.2. Gaseous absorption

Due to the presence of gas and water molecules in the atmosphere, electromagnetic wave travels more slowly, and part of its energy is scattered or absorbed. Some molecules present in a standard atmosphere are excited by the specific frequencies in the THz band. An excited molecule internally vibrates, and as a result of this vibration, part of the energy of the propagating wave is converted into kinetic energy and is simply lost. The necessary parameters to characterize the different resonances for different molecules are collected, contrasted with real measurements, and compiled into HITRAN database [18]. Considering the standard atmospheric composition (mostly molecular oxygen and nitrogen), the gaseous attenuation, γ_g (in dB/km), up to 0.350 THz (accurate model) and 1 THz (general model) can be evaluated using procedure described in [19]. For distances below 1 m, molecular absorption loss is considered to be almost negligible. When transmission distance exceeds 1 m, molecular resonances become significant.

3.2.1. Water vapor

More than any other region of the electromagnetic spectrum THz region is very vulnerable by water molecules. Being a polar molecule with a nonlinear molecular orientation, water displays a strong absorption line for nearly all of its rotational modes [20]. Therefore, it is worth to mention water vapor, which, being minor constituent of the atmosphere, together with oxygen, is the main contributor to gaseous attenuation. Hence, the gaseous attenuation, γ_g, is a sum of attenuation due to water vapor and oxygen, and the path loss due to atmospheric absorption is estimated as multiplication of gaseous attenuation and path length, d,

$$A_G = \gamma_g d. \tag{1}$$

In the molecular absorption spectrum, there are several regions of relative transparency between the absorption peaks. Those regions are called transmission windows. Under standard atmospheric conditions, transmission windows are present at about <0.300, 0.330–0.370, 0.390–0.440, 0.625–0.725, and 0.780–0.910 THz (**Figure 3**). When the frequency exceeds 1 THz, the radio wave undergoes significant absorption by water vapor and oxygen molecules in the

atmosphere [9]. In [21], an accurate terahertz time-domain spectroscopy (THz-TDS) characterization of water vapor from 0.2 to 2 THz was reported. The results agreed with the previously predicted and measured attenuations for the weak water lines, but showed more attenuation for the relatively transparent windows between these lines.

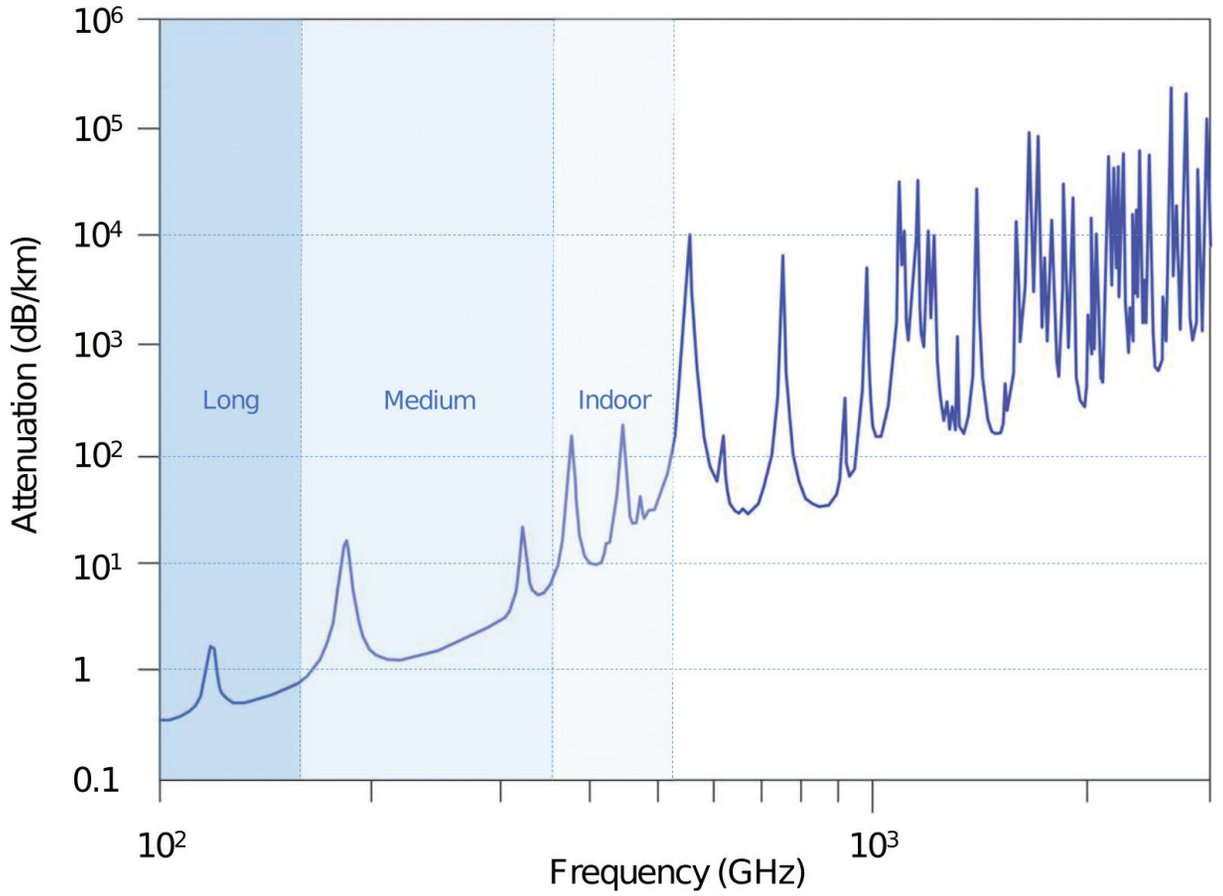

Figure 3. Transmission distance in the THz band is limited by the atmospheric attenuation. Water vapor absorption spectra indicate several transmission windows (the regions of relative transparency between the resonance peaks); when the frequency exceeds 1 THz, the radio wave undergoes significant absorption.

3.3. Precipitation

3.3.1. Rainfall

The effect due to hydrometeors, especially rain, is the most severe. The main mechanisms of the attenuation due to rainfall are absorption and scattering. When an incident electromagnetic wave passes over an object that has dielectric properties different from the surrounding medium, some energy is absorbed (this energy heats the absorbing material) and some is scattered (the smaller the scatterer, the more isotropic it is in direction with respect to the wavelength of the incident energy) [4]. It is a common practice to express the excess attenuation due to rainfall as a function of precipitation rate, which depends on liquid water content and the fall velocity of the raindrops, which in turn depends on drop size distribution (DSD). There are various raindrop size distributions; the most popular is the Laws and Parsons distribution. However, dealing with raindrop size distribution is a complex task, because the

shapes of actual raindrops are far from the usually depicted spherical or tear-drop shapes, as larger drops become flattened and eventually break into smaller droplets [22].

One of the most accepted methods of dealing with excess path attenuation due to rainfall is an empirical procedure based on the approximate relation between excess path attenuation A (in dB) and the rain rate R (in mm/h) [23]:

$$A_{dB} = a R^b, \tag{2}$$

where a and b are functions of frequency. Horizontally polarized waves suffer greater attenuation than vertically polarized waves, so there are different a and b values for vertical and horizontal polarization. The values of a and b can be found in [23].

For frequencies above 100 GHz, the attenuation is considered to be about 10 dB/km in the case of heavy-rain conditions (R = 25 mm/h). However, empirical methods must be applied with caution. Most often, the rain rate of the rainfall is calculated using averaged hourly, daily or even annual data. For path design above 10 GHz, where the path availability better than 99.9% is required, such averaged statistics are not sufficient, as several weeks of light drizzle will affect the overall long-term path availability much less than several good short-lived downpours [4]. In fact, such downpours are cellular in nature and appear in so-called rain cells. To trace such downpours, "one-minute" rain rate values, $R_{(1\,\mathrm{min})}$ (in mm/h), are required. Since data with such accuracy are rarely collected, the "one-minute" rain rate values (integration time is 1 min) can be estimated from various models [16]. However, those models are also based on averaged data; therefore, in territories of varying climate conditions, it is suggested to specify the conversion formula in accordance with the peculiarities of the climate. As the practice shown, the actual "one-minute" rain rate values tend to be higher than the ITU-R suggested values, and it is the main reason for the unexpected telecommunication failures during downpours.

3.3.2. Other precipitation

There are other meteorological phenomena. In example, hail causes only a small attenuation due to rain. The effect of snow depends on temperature, flake size, and water content. Fog and clouds can be treated as very light rains (small droplets or/and ice crystals). In this chapter, other precipitation sources will not be discussed. More information can be found in [4, 16].

3.4. Variations of the atmospheric refractive index

In the atmosphere, the propagating radio beam encounters variations of the atmospheric refractive index. Due to these variations, the ray-path becomes curved, and the fading occurs. The radio refractive index is defined as the ratio of the velocity of propagation of a radio wave in free space to the velocity in a specified medium. At standard atmosphere conditions near the Earth's surface, the radio refractive index has a value of approximately 1.0003. The atmospheric refractive index, n, can be calculated by the following formula:

$$n = 1 + N \times 10^{-6}, \tag{3}$$

where N is the atmospheric refractivity.

According to the procedure described in [4], the atmospheric refractivity is expressed by:

$$N = \frac{77.6}{T}\left(P + 4810\,\frac{e}{T}\right), \tag{4}$$

where P is atmospheric pressure (in hPa), e is water vapor pressure (in hPa) and T is absolute temperature (in K). This expression may be used for all radio frequencies (with the error less than 0.5% for frequencies up to 100 GHz).

The water vapor pressure is given by

$$e = \frac{H e_s}{100}, \tag{5}$$

$$e_s = a \exp\left(\frac{bt}{t + c}\right), \tag{6}$$

where H is relative humidity (in %), t is temperature (in °C), e_s is saturation vapor pressure (in hPa) at the temperature t (in °C), and the coefficients a, b, c are a = 6.1121, b = 17.502, c = 240.97 (for water, valid between −20°C and +50°C, with an accuracy of ±0.20%) and a = 6.1115, b = 22.452, c = 272.55 (for ice, valid between −50°C and 0°C, with an accuracy of ±0.20%).

4. Simulations using real-time data

The main challenge of the radio system design is the reliable source of data. When dealing with atmospheric attenuation, it is very important to gather as reliable as possible metrological data. Unfortunately, data of such accuracy are rarely available. In this part, simulations based on real-time data are presented.

4.1. Rain rate integration time problem

As mentioned above, the mostly available meteorological data are not sufficient for the radio system design, as averaged meteorological data suppress the peak values of significant events, such as downpours. Therefore, 1-min integration time should be used if available.

In **Figure 4**, the data of the heavy-rain event are presented. During 6-h lapse, the rain intensity differed from light to heavy rain, and 37 mm of rain was accumulated until midnight (marked as Precip. Accum.). At the same time, the rain intensity was measured (R-value (10 min)). For technical reasons, the measurements were carried out in 10-min intervals. In addition, 1-min rain rate value, $R_{(1\,\mathrm{min})}$, was calculated, using the Moupfouma and Martin method [24]:

$$R_{(1\,\mathrm{min})} = \left(R_{(\tau_{\mathrm{min}})}\right)^{0.987\tau^{0.061}}, \tag{7}$$

where $R_{(\tau_{\mathrm{min}})}$ is the rain rate value (in mm/h) measured in lapse of time τ (in minutes).

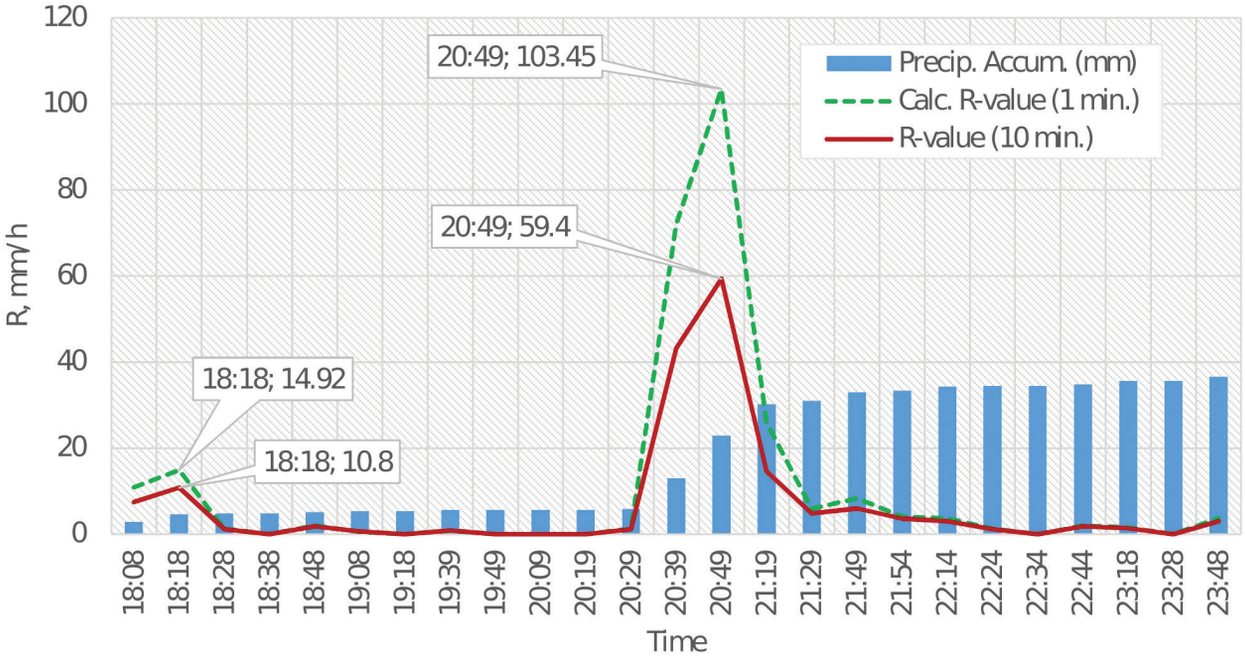

Figure 4. Heavy-rain event. The peak values of the rain rate at the different aggregation times are presented. According to measurements, the maximum *R*-value was *R* = 59.4 mm/h at 20:49; the maximum calculated 1-min *R*-value was almost double, *R* (1 min)=103.45 mm/h. Both of these values are higher than the ITU-R suggested value *R* = 35 mm/h.

According to measurements, the maximum *R*-value was *R* = 59.4 mm/h at 20:49. However, calculated 1-min *R*-value was almost double, $R_{(1\text{min})}$ = 103.45 mm/h. Both of these values are higher than the ITU-R suggested value *R* = 35 mm/h [25].

In **Figure 5**, calculated values of rain attenuation at 0.1 THz (or 100 GHz; the minima of the THz range) electromagnetic waves are presented. As can be seen, the results are different for 1- and 10-min integration times. One-minute rain rate value reveals the peak attenuation being 32.27 dB/km for horizontally polarized electromagnetic waves and 31.55 dB/km for vertically polarized ones. The values calculated using 10-min integration time are lower (22.11 and 21.02 dB/km, respectively). However, when the rain rate starts to fall, the integration time and polarization become less important, as the results in all cases are nearly similar.

In **Figure 6**, the same rain event is presented. The difference is that the *R*-values were calculated using more widely accessible averaged rainfall data with integration time of 1 h and 6 h (standard). In these cases, the downpours are suppressed and delayed (*R* = 24.6 mm/h at 21:19 according to hourly data; *R* = 6.56 mm/h at 23:18 according to 6-h average data).

As can be seen in **Figure 7**, the impact of the suppressed and delayed *R*-values on the attenuation of the propagating 0.1 THz electromagnetic waves is significant and the results are distorted in comparison with the **Figure 5**. The low attenuation values become higher, and the peak values are lower (12.13 dB/km for horizontally polarized waves in comparison with 32.27 dB/km in **Figure 5**). The 6-h (standard) *R*-values (see inset in **Figure 7**) determine very low and delayed attenuation values.

The same calculations were performed for electromagnetic waves with operating frequency of 0.3 THz (or 300 GHz; in many cases, this frequency is considered as a realistic candidate

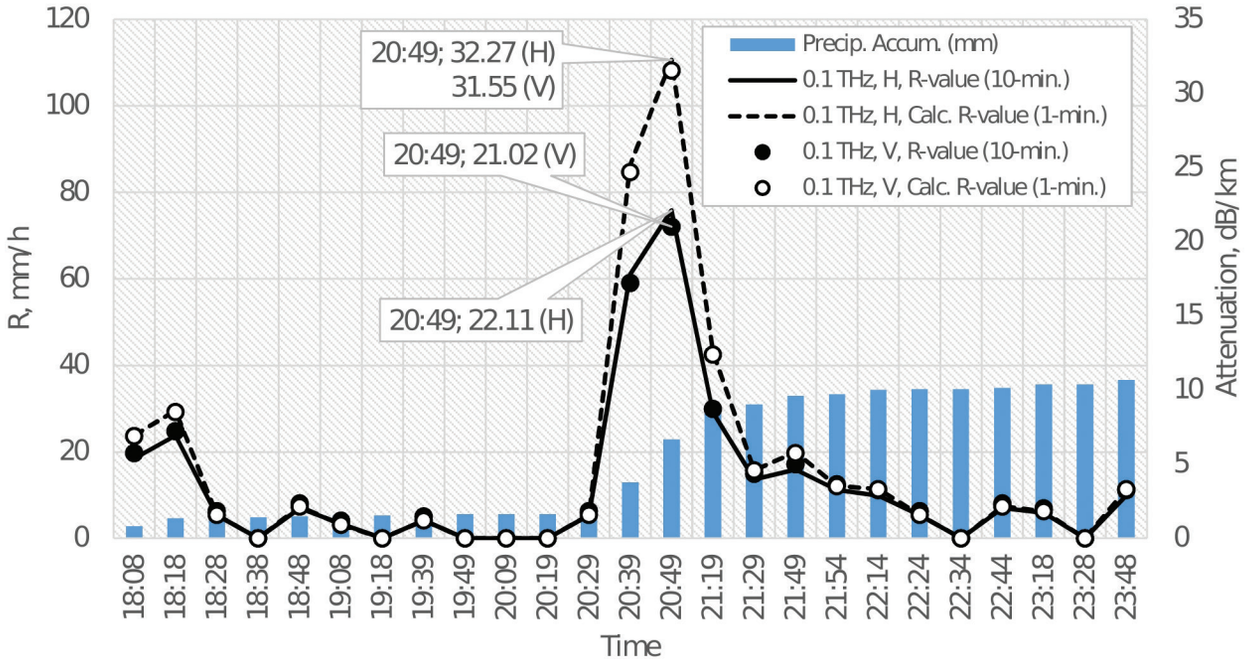

Figure 5. The calculated values of rain attenuation at 0.1 THz using real-time *R*-values. The results differ with integration time. One-minute rain rate value reveals the peak attenuation being 32.27 dB/km for horizontally polarized electromagnetic waves and 31.55 dB/km for vertically polarized ones when the rain rate is 103.45 mm/h.

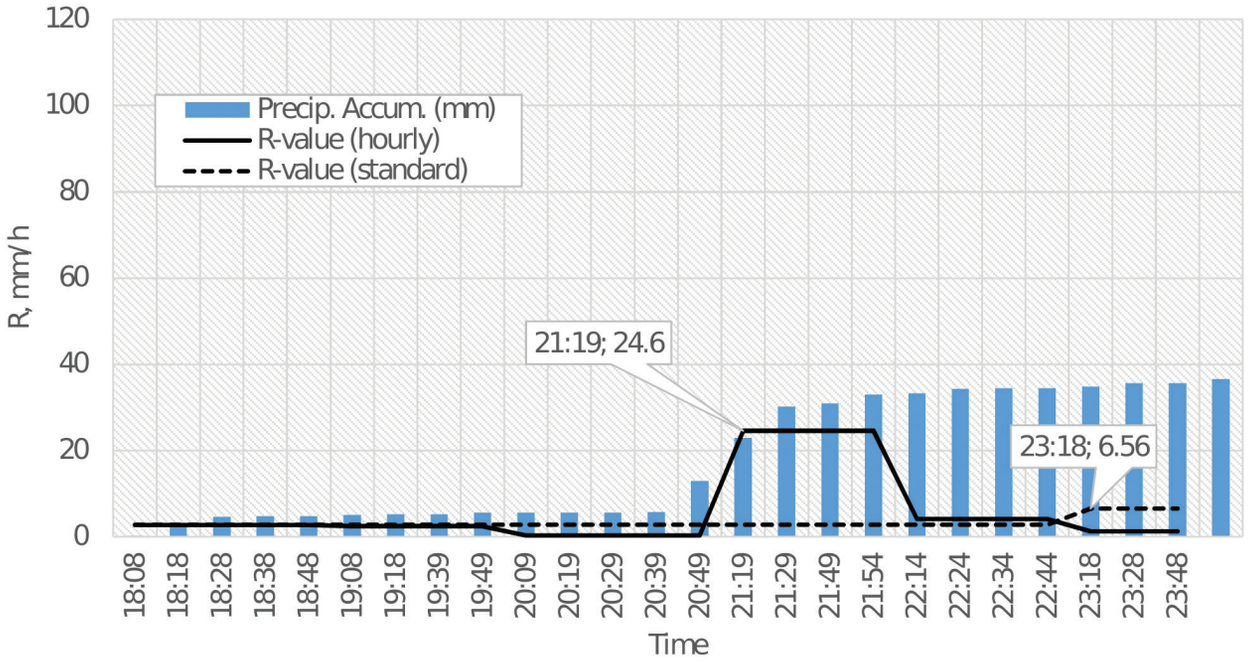

Figure 6. The *R*-values calculated using averaged hourly meteorological data. The downpours are suppressed and delayed in comparison with **Figure 4**.

for the THz communications). The results are presented in **Figure 8**. As can be seen, the tendencies are the same as for 0.1 THz. However, for 0.3 THz, the calculated attenuation values are smaller than for 0.1 THz (according to model, for frequencies higher than 0.1 THz, the rain attenuation slightly decreases) (**Figure 9**).

http://dx.doi.org/10.5772/intechopen.72205

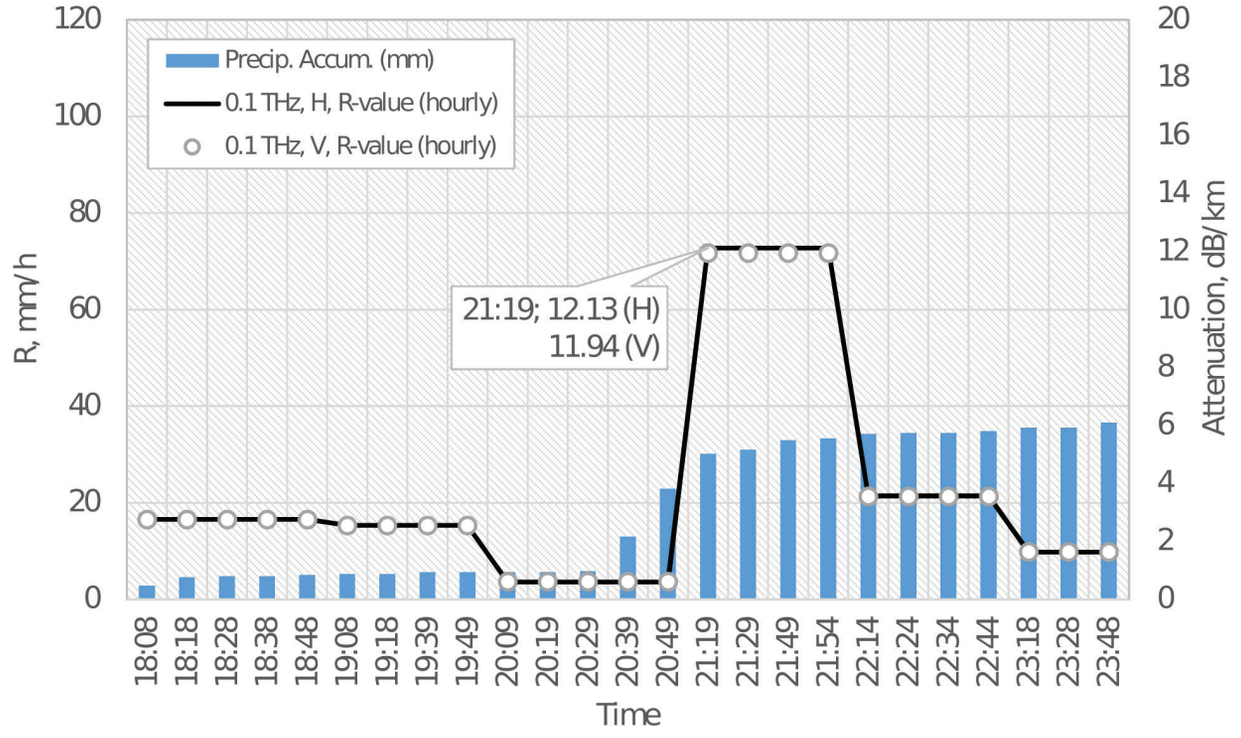

Figure 7. The calculated values of rain attenuation at 0.1 THz using averaged *R*-values. The results are distorted, as the low attenuation values are higher and the peak values are lower.

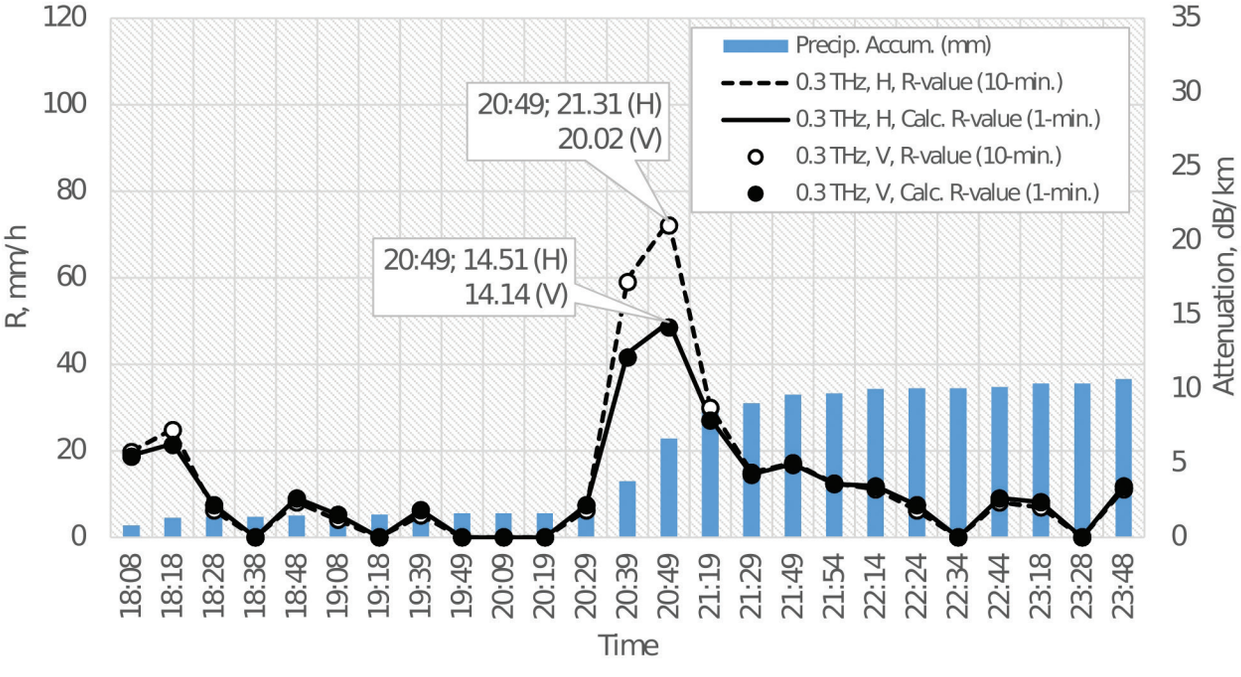

Figure 8. The calculated values of rain attenuation at 0.3 THz. For 0.3 THz, the attenuation values are smaller than for 0.1 THz, but the tendencies are the same.

4.2. Atmospheric refractivity

The atmospheric refractivity, *N*, defines the curvature of the ray path due to which the fading occurs. Since the *N*-value is frequency independent (see formula (4)), the main peculiarities

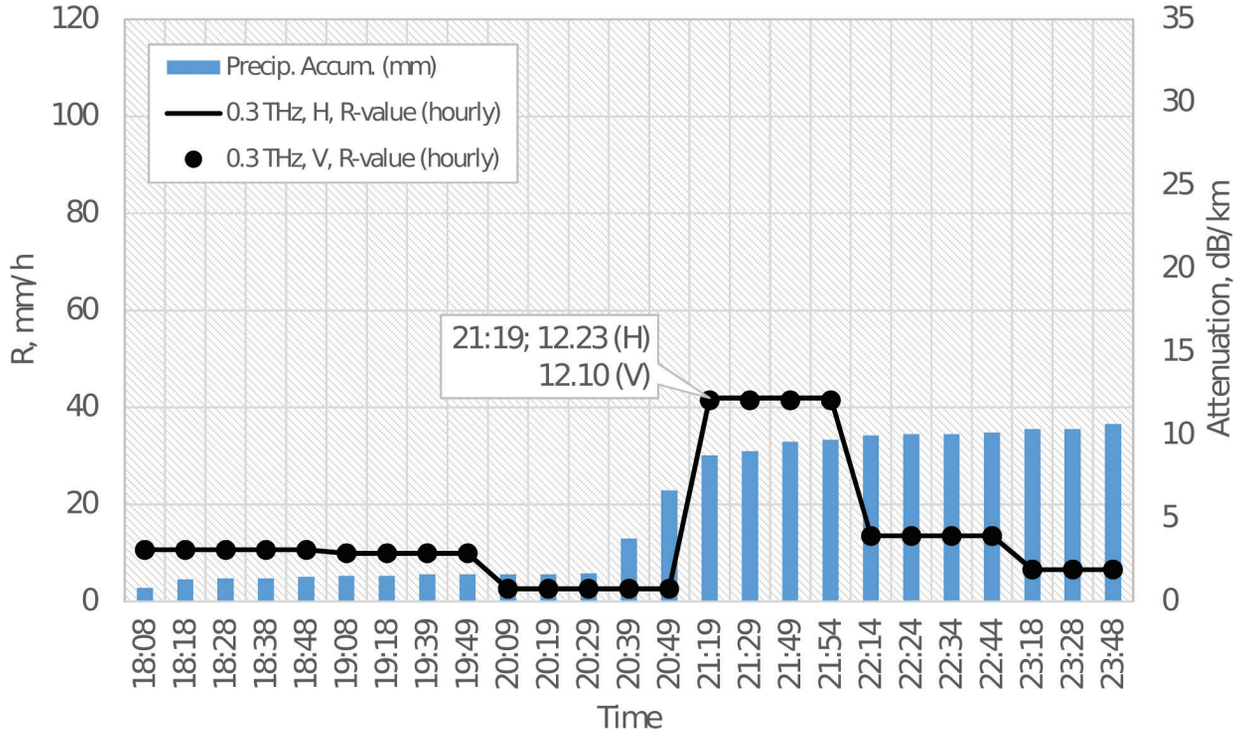

Figure 9. The calculated values of rain attenuation at 0.3 THz using averaged *R*-values. The results are distorted, as the low attenuation values are higher and the peak values are lower.

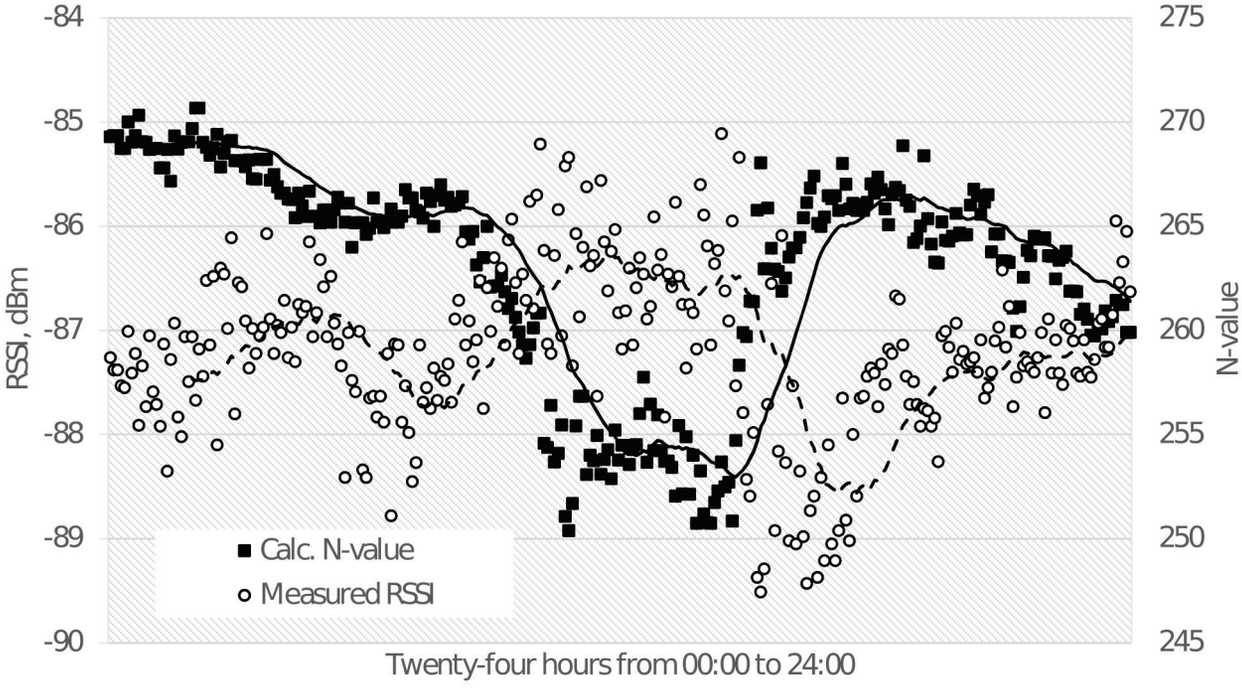

Figure 10. Variations of radio refractivity compared to measured signal strength. Changes of the signal strength occurred at same time as the variations of the radio refractivity. Since the *N*-value is frequency independent (see formula (4)), the main peculiarities can be identified using measurements performed for lower operating frequencies.

can be identified using measurements performed at lower operating frequencies. In **Figure 10**, the actual measurements of the signal (working frequency 3.5 GHz) are presented. The measurements were carried out in the area of weak radio coverage. The measurements are compared to the *N*-values, calculated using (4) formula and real-time meteorological data, which was measured at the same place. As can be seen, changes of the signal strength occur at same time as the variations of the radio refractivity (please note that the scale is chosen for the convenience of viewing the regularities).

5. Conclusions

In this chapter, the challenges of the very promising ultrabroadband terahertz (THz) wireless networks in terms of the atmospheric attenuation and atmospheric refractivity are presented. The main mechanisms of the atmospheric attenuation are briefly discussed. The simulations, based on the real-time measurements and reliable meteorological data, are presented as well. As most of the atmospheric attenuation mechanisms are quite well predictable or can generally be neglected, the causes of the hardest-to-predict failures are the events of heavy rain (the THz waves are vulnerable by the water molecules) and variations of atmospheric radio refractivity. These simulations are focused on the lower THz band, but could also be applicable for other operating frequencies.

Simulations show that in the events of heavy rain the actual peak values of the rain rate can be twice as high as the peak values calculated using meteorological data, collected with the 10-min integration time. As a result, averaged meteorological data gives inaccurate and distorted results, as the peak values are suppressed and delayed.

The curvature of the ray-path is determined by the atmospheric refractivity. Since the formula of atmospheric refractivity is frequency independent (for frequencies up to 0.1 THz, the error is less than 0.5%), the main peculiarities can be identified using measurements performed for lower operating frequencies. Some initial measurements are presented. The results show that the changes of the signal strength occur at same time as the variations of the atmospheric radio refractivity. Those variations might be very influential in the areas of the weak coverage.

Simulations of the atmospheric attenuation using real-time data are a powerful tool that should complement technological basis, as it will help to foresee possible failures, extend transmission distance and improve reliability of the THz and other high-frequency broadband wireless networks.

Author details

Milda Tamosiunaite[1]*, Stasys Tamosiunas[2], Mindaugas Zilinskas[2,3] and Gintaras Valusis[1,2]

*Address all correspondence to: milda.tamosiunaite@ftmc.lt

1 Center for Physical Sciences and Technology, Vilnius, Lithuania

2 Faculty of Physics, Vilnius University, Vilnius, Lithuania

3 Communications Regulatory Authority of the Republic of Lithuania, Vilnius, Lithuania

References

[1] Cherry S. Edholm's law of bandwidth. IEEE Spectrum. 2004;**41**(7):58-60. DOI: 10.1109/MSPEC.2004.1309810

[2] Cisco. The Zettabyte Era: Trends and Analysis [Internet]. [Updated: June 7, 2017]. Available from: https://www.cisco.com/c/en/us/solutions/collateral/service-provider/visual-networking-index-vni/vni-hyperconnectivity-wp.html [Accessed: 20-09-2017]

[3] Shannon CE. A mathematical theory of communication. The Bell System Technical Journal. 1948;**27**(3):379-423, 623-656. DOI: 10.1002/j.1538-7305.1948.tb01338.x

[4] Roger L. Freeman. Radio System Design for Telecommunication. 3rd ed. Wiley-IEEE Press; 2007. 912 p

[5] Tonouchi M. Cutting-edge terahertz technology. Nature Photonics. 2007;**1**:97-105. DOI: 10.1038/nphoton.2007.3

[6] Kawase K, Ogawa Y, Watanabe Y, Inoue H. Non-destructive terahertz imaging of illicit drugs using spectral fingerprints. Optics Express. 2003;**11**(20):2549-2554. DOI: 10.1364/OE.11.002549

[7] Akyildiz IF, Jornet JM, Hana C. Terahertz band: Next frontier for wireless communications. Physical Communication. 2014;**12**:16-32. DOI: 10.1016/j.phycom.2014.01.006

[8] Ishigaki K et al. Direct intensity modulation and wireless data transmission characteristics of terahertz-oscillating resonant tunnelling diodes. Electronics Letters. 2012;**48**(41):582. DOI: 10.1049/el.2012.0849

[9] Nagatsuma T, Ducournau G, Renaud CC. Advances in terahertz communications accelerated by photonics. Nature Photonics. 2016;**10**:371-379. DOI: 10.1038/nphoton.2016.65

[10] Koenig S et al. Wireless sub-THz communication system. Nature Photonics. 2013;**7**:977-981. DOI: 10.1038/nphoton.2013.275

[11] Hoydis J et al. Massive MIMO in the UL/DL of cellular networks: How many antennas do we need? IEEE Journal on Selected Areas in Communications. 2013;**31**(2):160-171. DOI: 10.1109/JSAC.2013.130205

[12] Ge X et al. 5G ultra-dense cellular networks. IEEE Wireless Communications. 2016; **23**(1):72-79. DOI: 10.1109/MWC.2016.7422408

[13] Akyildiz IF. Enabling next generation small cells through femtorelays. Physical Communication. 2013;**9**:1-15. DOI: 10.1016/j.phycom.2013.04.001

[14] Barros MT, Mullins R. Integrated terahertz communication with reflectors for 5G small-cell networks. IEEE Transactions on Vehicular Technology. 2016;**66**(7):5647-5657. DOI: 10.1109/TVT.2016.2639326

[15] Kleine-Ostmann T, Nagatsuma T. A review on terahertz communications research. Journal of Infrared, Millimeter, and Terahertz Waves. 2011;**32**(2):143-171. DOI: 10.1007/s10762-010-9758-1

[16] Tamosiunaite M et al. Atmospheric attenuation due to Humidity. In: Zhurbenko V, editor. Electromagnetic Waves. InTech; 2011. DOI: 10.5772/21430

[17] Internation Telecommunication Union. P.525: Calculation of free-space attenuation [Internet]. 2016. Available from: https://www.itu.int/rec/R-REC-P.525/en [Accessed: 01-09-2017]

[18] HITRAN database. Available from: http://hitran.org/ [Accessed: 15-09-2017]

[19] Internation Telecommunication Union. P.676: Attenuation by atmospheric gases [Internet]. 2016. Available from: https://www.itu.int/rec/R-REC-P.676/en [Accessed: 01-09-2017]

[20] Brown E. Fundamentals of terrestrial millimeter-wave and THz remote sensing. International Journal of High Speed Electronics and Systems. 2011;**13**(4):1-106. DOI: 10.1142/S0129156403002125

[21] Yang Y, Shutler A, Grischkowsky D. Measurement of the transmission of the atmosphere from 0.2 to 2 THz. Optics Express. 2011;**19**(9):8830-8838. DOI: 10.1364/OE.19.008830

[22] Villermaux E, Bossa B. Single-drop fragmentation determines size distribution of raindrops. Nature Physics. 2009;**5**:697-702. DOI: 10.1038/nphys1340

[23] International Telecommunication Union. P.838: Specific attenuation model for rain for use in prediction methods [Internet]. 2005. Available from: https://www.itu.int/rec/R-REC-P.838/en [Accessed: 01-09-2017]

[24] Moupfouma F, Martin L. Modelling of the rainfall rate cumulative distribution for the design of satellite and terrestrial communication systems. International Journal of Satellite Communications and Networking. 1995;**13**(2):105-115. DOI: 10.1002/sat.4600130203

[25] International Telecommunication Union. P.837: Characteristics of precipitation for propagation modelling [Internet]. 2017. Available from: https://www.itu.int/rec/R-REC-P.837/en [Accessed: 05-09-2017]

IntechOpen